

Copyright (2006) American Institute of Physics. This article may be downloaded for personal use only. Any other use requires prior permission of the author and the American Institute of Physics.

The following article appeared in Appl. Phys. Lett. 89, 071110 (2006) and may be found at [http://apl.aip.org/applab/v89/i7/p071110\\_s1?isAuthorized=no](http://apl.aip.org/applab/v89/i7/p071110_s1?isAuthorized=no)

## Tunable silicon microring resonator with wide free spectral range

Magdalena S. Nawrocka,<sup>a)</sup> Tao Liu, Xuan Wang, and Roberto R. Panepucci  
 Department of Electrical and Computer Engineering, Florida International University,  
 10555 West Flagler Street, Miami, Florida 33174

(Received 13 March 2006; accepted 28 June 2006; published online 17 August 2006)

The authors present a silicon-on-insulator single ring resonator with a free spectral range equal to 47 nm, which is the widest known value for this type of resonators. The ring radius is 2  $\mu\text{m}$  and is the smallest ring resonator ever reported, achieving experimentally such a wide spectral range. For this ring resonator, the authors demonstrate the quality factor to be equal to  $6730 \pm 60$ . They thermally tune the resonant wavelength with  $0.11 \text{ nm}/^\circ\text{C}$ , thus showing the ring resonator as an attractive component for on-chip ultracompact photonic add/drop filters and switches. © 2006 American Institute of Physics. [DOI: 10.1063/1.2337162]

Microring resonators are considered to be multifunctional photonic components for all-optical circuits. They can be used as building blocks for all-optical wavelength switches,<sup>1</sup> converters,<sup>2</sup> high-speed tunable filters, add-drop multiplexers,<sup>3</sup> ultrafast switches,<sup>4</sup> laser cavities, notch filters,<sup>5</sup> and perhaps as convenient calibration references for optical spectrum analyzers and wave division multiplexing networks.<sup>6</sup> In addition to telecommunications, ring resonators show potential to be applied as nonlinear optical devices<sup>7</sup> and as elements of lab-on-chip devices for biosensing.<sup>8</sup> Our interest arises from the need for on-chip waveguide sensor multiplexing. In this case, different wavelengths are used to address individual elements on a sensor array.

Silicon is a leading material in micro-optoelectronics and its well known technology makes silicon-on-insulator (SOI) photonic devices potentially low cost and compatible with existing silicon microelectronics. Because of the large refractive index difference between Si ( $n \approx 3.5$ ) and  $\text{SiO}_2$  ( $n \approx 1.5$ ), the SOI technology allows creation of submicrometer single-mode waveguides. This ensures ultrahigh light confinement leading to compact photonic devices with sharp bends, making possible large scale photonic integration.<sup>9</sup> Finally, silicon microphtonics is expected to become inexpensive due to its complementary metal-oxide semiconductor compatible fabrication techniques, and therefore is particularly suitable for sensors.

Many applications need wide spacing between resonant wavelength peaks, which require a wide free spectral range (FSR). A large FSR enables the multiplexing of a large number of devices. A suitable spectral range would match that of the readily available gain spectra of erbium-doped optical amplifiers. The most common devices with wide FSR are based on complex microelectromechanical and liquid crystal etalons or lattice devices,<sup>10</sup> which are difficult to integrate on photonic chips. Recently, a hybrid integrated filter consisting of a silver-coated thin film of lithium niobate on SOI has been reported with FSR equal to 53.2 nm, but its full width at half maximum (FWHM) was 5 nm.<sup>11</sup> The chip area needed for this resonator was between 250 and 500  $\mu\text{m}^2$ . We describe an ultrasmall SOI ring resonator with ring radius equal to 2  $\mu\text{m}$ . The area occupied by our resonator with

lead-in and lead-out waveguides in the coupling region is below 30  $\mu\text{m}^2$  and it is comparable with that needed for the reported smallest photonic crystal cavities.<sup>12</sup> This indicates that silicon microring resonators are suitable components for ultracompact photonic devices.

The ring resonators presented here were fabricated on a SOI wafer with a 3  $\mu\text{m}$  buried oxide layer by electron-beam lithography, followed by inductively coupled plasma etching and the deposition of a 1- $\mu\text{m}$ -thick  $\text{SiO}_2$  cladding by plasma-enhanced chemical-vapor deposition. The devices were fabricated in a single lithographic step, resulting in structures that laterally couple light through an evanescent-wave interaction. A waveguide for buses and resonators with nominal width of 450 nm and height of 250 nm was chosen for single-mode operation at wavelength  $\lambda = 1550 \text{ nm}$ . The resonators, formed of bent single-mode waveguides with 2  $\mu\text{m}$  radius, have distances between ring and coupling waveguides of 100, 200, and 300 nm. Input/throughput port and add/drop port waveguides were added to each ring as seen in the inset in Fig. 1. This configuration allowed measurement of backscattered light in addition to light coupled to the drop port. The nominal distance between the

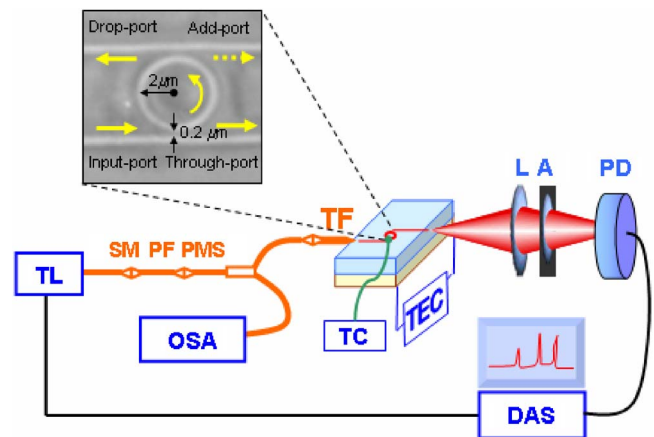


FIG. 1. (Color online) Experimental setup for the measurement of ring resonator's parameters. Inset: Optical image of ring resonator with description of ports and directions of light propagation. (TL) tunable laser, (SM) single mode fiber with polarization controller, (PF) fiber-optic in-line polarizer, (PMS) polarization maintaining fiber-optic splitter, (TF) polarization maintaining tapered fiber, (L) objective lens, (A) analyzer, (PD) photodetector, (TC) thermocouple, (TEC) thermoelectric controller, (OSA) optical spectrum analyzer, and (DAS) data acquisition system.

<sup>a)</sup>Electronic mail: nawrocka@fiu.edu

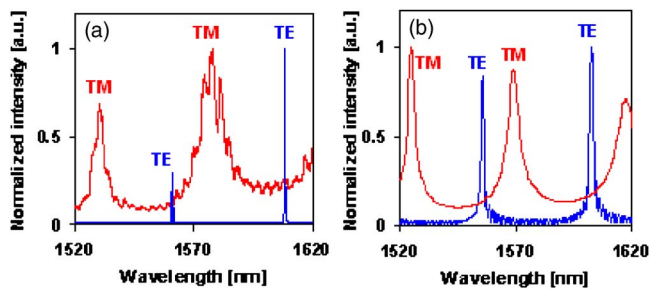


FIG. 2. (Color online) (a) Measured and (b) calculated resonance peaks of TE and TM modes.

2- $\mu\text{m}$ -radius ring described here and the coupling waveguides is 200 nm.

Characterization of the devices was carried out with an Ando 4613D tunable laser (wavelength range from 1520 to 1620 nm and wavelength step of 1 pm) using the setup schematically presented in Fig. 1. Light from the tunable laser was coupled with a polarization-maintaining tapered fiber into the SOI nanotapered input waveguide.<sup>13</sup> To investigate the polarization response, light from the laser was coupled through a polarization controller to a fiber-optic in-line polarizer, followed by a 90/10 polarization-maintaining fiber-optic splitter to allow monitoring of laser output. Since silicon waveguides are polarization sensitive, it is important to control the state of polarization. Application of the nanotapered waveguide improves coupling efficiency of light by matching size, profile, and effective index of the propagating light mode at the expense of polarization-dependent insertion loss, which is a strong function of nanotaper dimensions.<sup>13</sup> The light coming out from the drop/through/add ports was coupled through the objective lens and polarization analyzer to a photodiode. The signal was then collected by a LABVIEW data control/acquisition system.

We measured the spectral characteristics of the ring resonators for both linear polarizations TE (parallel to the chip surface) and TM (perpendicular to the chip surface) of the fundamental mode. Figure 2(a) shows the normalized optical power measured at the drop port of the device, after coupling from the input waveguide, through the ring resonator. Incoming light was polarized at  $0^\circ$  and then  $90^\circ$ , leading to excitation of TE mode and then TM mode at the input. Narrow resonance characteristics occurred for the TE polarization, while the TM mode shows broader resonance peaks due to its weaker confinement in the waveguide core and higher coupling efficiency to the resonator over a wider wavelength range. Simulations carried out with the three-dimensional finite-difference time domain method [Fig. 2(b)] confirm the broadening of TM mode. Figure 3(a) shows the spectral characteristic of the drop port for TE polarization. From the figure, the free spectral range of the device is equal to 47 nm. This is the widest FSR ever demonstrated experimentally for a single SOI ring resonator. Furthermore, the FWHM of the resonance peak at  $\lambda=1608.249$  nm was fitted to a Lorentzian curve and was determined to be  $0.239 \pm 0.002$  nm, which results in a quality factor  $Q=6730 \pm 60$ . This value of  $Q$  factor is  $\sim 5\%$  lower than the maximum theoretical value reported in Ref. 14. The separation gap between resonator and waveguides influences the peak width—a wider gap allows achieving narrower FWHM [see Fig. 3(a)]. However, an excessively wide gap decreases the coupling from waveguide to resonator, thus a compromise has to be reached to fulfill

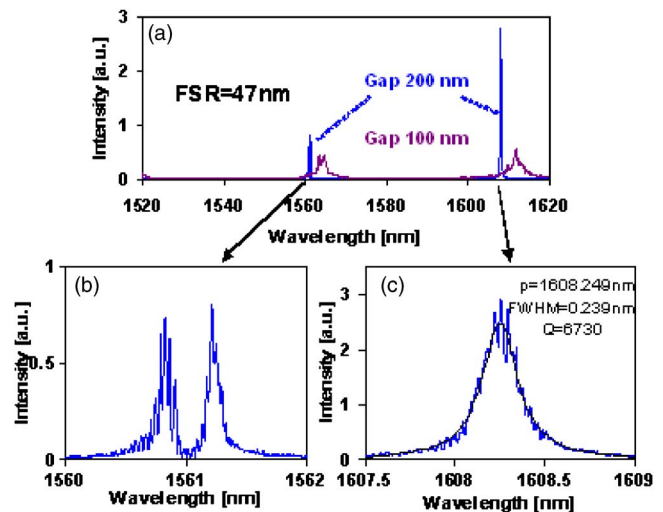


FIG. 3. (Color online) (a) Spectral characteristics measured from the drop port for ring resonators with different separation gaps. (b) Splitting of resonance caused by the roughness of waveguide walls. (c) Resonance peak with the superimposed waveguide oscillations.

both conditions. In the present case, the highest power at the drop-port output occurred for the gap separation of 200 nm. The peak-to-background signal ratio in this case was 20 dB as seen in Fig. 3(a). Coupling through the ring on the device with a gap separation of 300 nm could not be detected either on the drop port or in the presence of dips of light on the through port. An occurrence of double peak at  $\lambda=1561$  nm can be explained by the roughness of the waveguide walls that lifts the degeneracy of forward and backward traveling modes of a resonating wave.<sup>15</sup> Additional oscillations superimposed on the resonance peak [Fig. 3(c)] originate from the add/drop waveguide of length  $15 \pm 3$  mm that acts as a Fabry-Pérot resonator. Based on the measured FSR = 0.04 nm of the oscillations, the calculated Fabry-Pérot cavity length is  $18 \pm 4$  mm. Comparison of measured and calculated cavity lengths confirms that the add/drop waveguide produces the oscillations.

In order to explore thermal effects, we measured the spectral characteristics as a function of temperature, by heating/cooling the whole chip, using a thermoelectric Peltier element attached to the bottom of the chip. After every change of temperature, when the chip reached thermodynamic equilibrium, the measurement was taken with the use of a thermocouple attached to the top of the chip. As shown in Fig. 4, we determined the linear resonance shift to be equal to  $0.11$  nm/ $^\circ\text{C}$ . The main contribution to this thermal shift is due to the thermo-optic effect in silicon ( $\Delta n/\Delta T \approx 1.9 \times 10^{-4}/^\circ\text{C}$ ).<sup>16</sup> Assuming that the effective index for

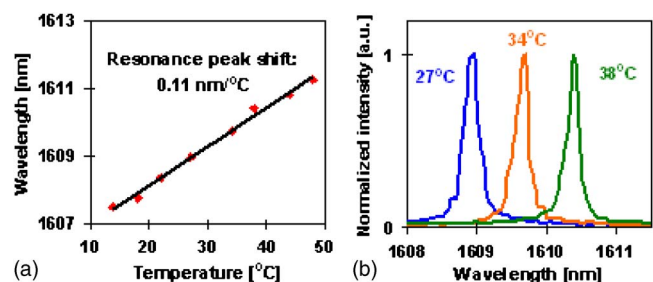


FIG. 4. (Color online) (a) Thermal characteristic of ring resonator. (b) Examples of resonance peak shift for three different temperatures.

TE mode is  $n \approx 2.5$ , the thermal peak shift was expected to be  $0.12 \text{ nm}/^\circ\text{C}$ , according to the formula

$$\Delta\lambda_T = \lambda \frac{\Delta n}{\Delta T n}. \quad (1)$$

This reasoning is confirmed by reported measurement of similar, but three times larger silicon ring resonator, for which the thermal resonance shift is determined to be  $0.1 \text{ nm}/^\circ\text{C}$ .<sup>17</sup>

In conclusion, we experimentally realized a single SOI ring resonator add/drop filter with the widest known FSR = 47 nm. With such a large FSR it is possible to use large arrays of devices for multiplexing applications and provide gain through the whole spectrum of an erbium-doped amplifier. This large FSR was achieved through the use of a single ring resonator with a radius of  $2 \mu\text{m}$ . We achieved a  $Q$  factor of  $6730 \pm 60$  and  $\text{FWHM} = 0.239 \pm 0.002 \text{ nm}$ . One of the challenges lies in minimizing the roughness of waveguide walls, which will allow realization of a device with a single narrow peak at  $\lambda = 1561 \text{ nm}$ . The area needed for this resonant structure was only  $30 \mu\text{m}^2$ , which can lead to large integration of optical devices. We also demonstrate that local heating of resonators will make it possible to tune the devices and even build a wavelength-selective switch. The ring resonator presented here is a serious candidate for ultracompact photonic circuits and a milestone towards on-chip ultrahigh capacity all-optical network.

This work was supported by National Science Foundation Award No. 0446571 and Air Force Office of Scientific

Research Award No. FA9550-05-1-0232. The authors are thankful to Vilson R. Almeida for very helpful discussion.

<sup>1</sup>V. R. Almeida, C. A. Barrios, R. R. Panepucci, and M. Lipson, *Nature (London)* **431**, 1081 (2004).

<sup>2</sup>Q. Xu, V. R. Almeida, and M. Lipson, *Opt. Lett.* **30**, 2733 (2005).

<sup>3</sup>S. T. Chu, B. E. Little, W. Pan, T. Kaneko, and J. Kokubun, *IEEE Photonics Technol. Lett.* **11**, 1423 (1999).

<sup>4</sup>S. Gulde, A. Jebali, and N. Moll, *Opt. Express* **13**, 9502 (2005).

<sup>5</sup>P. P. Absil, J. V. Hryniewicz, B. E. Little, R. A. Wilson, L. G. Joneckis, and P. T. Ho, *IEEE Photonics Technol. Lett.* **12**, 398 (2000).

<sup>6</sup>S. L. Gilbert, S. M. Etzel, and W. C. Swann, *Optical Fiber Communications Conference (OFC), Postconference Technical Digest (2002)*, Vol. 1, pp. 391–393.

<sup>7</sup>V. R. Almeida and M. Lipson, *Opt. Lett.* **29**, 2387 (2004).

<sup>8</sup>A. Yalcin, K. C. Popat, J. C. Aldridge, T. A. Desai, J. Hryniewicz, N. Chbouki, B. E. Little, O. King, V. Van, S. Chu, D. Gill, M. Anthes-Washburn, M. S. Umlu, and B. B. Goldberg, *IEEE J. Sel. Top. Quantum Electron.* **12**, 148 (2006).

<sup>9</sup>R. A. Soref, *Thin Solid Films* **294**, 325 (1997).

<sup>10</sup>K. Yamada, T. Shoji, T. Tsuchizawa, T. Watanabe, J. Takahashi, and S. Itabashi, *Opt. Lett.* **28**, 1663 (2003).

<sup>11</sup>R. M. Roth, T. Izuhara, R. L. Espinola, D. Djukic, R. M. Osgood, Jr., S. Bakhru, and H. Bakhru, *Opt. Lett.* **30**, 994 (2005).

<sup>12</sup>Y. Akahane, T. Asano, B.-S. Song, and S. Noda, *Nature (London)* **425**, 944 (2003).

<sup>13</sup>V. R. Almeida, R. R. Panepucci, and M. Lipson, *Opt. Lett.* **28**, 1302 (2003).

<sup>14</sup>C. Manolatou and M. Lipson, *J. Lightwave Technol.* **24**, 1433 (2006).

<sup>15</sup>B. E. Little and J. P. Laine, *Opt. Lett.* **22**, 4 (1997).

<sup>16</sup>G. Cocorullo, F. G. Della Corte, and I. Rendina, *Appl. Phys. Lett.* **74**, 3338 (1999).

<sup>17</sup>V. Padgaonkar, The 2004 NNIN REU Research Accomplishments, 2004, pp. 98–99 (unpublished), <http://www.nnin.org/doc/2004NNINreuRA.pdf>